The Holocene isotopic record of aquatic cellulose from Lake Äntu Sinijärv, Estonia: influence of changing climate and organic-matter sources

F. Alayne Street-Perrott[a], Jonathan A. Holmes[b], Iain Robertson[a], Katherine J. Ficken[a], Tiiu Koff[c], Neil J. Loader[a], Jim D. Marshall[d], Tõnu Martma[e].

[a]Department of Geography, College of Science, Swansea University, Swansea, SA2 8PP, UK.
[b]Environmental Change Research Centre, Department of Geography, University College London, Gower Street, London, WC1E 6BT, UK.
[c]Institute of Ecology, Tallinn University, Uus-Sadama 5, 10120, Tallinn, Estonia.
[d]Department of Earth, Ocean and Ecological Sciences, University of Liverpool, Liverpool, L69 3GP, UK.
[e]Department of Geology, Tallinn University of Technology, Ehitajate tee 5, 19086 Tallinn, Estonia.

Supplementary Data

1. Extended methods

1.1 Field methods

Total monthly precipitation was collected approximately monthly between October 2004 and December 2006 in a modified rainfall collector following IAEA GNIP protocols (IAEA, 2014). Groundwater was sampled from a nearby well on six occasions between May 2005 and March 2006. Lake-water samples were collected from close to the lake centre, approximately monthly between March 2004 and March 2006. On most occasions, a surface sample and a depth profile were collected. Samples of snow and meltwater were also retrieved from the frozen lake surface on several occasions during winter (sample locations are shown in Fig. 1 in the main manuscript).

Lake sediments were recovered from 4.1m of water by coring through the ice using a Russian corer: two overlapping cores (ANTU1 and ANTU2), which were taken within one metre of each other, were required to retrieve the entire Holocene sequence. Cores were generally recovered in 1m lengths, extruded in the field into PVC pipes, wrapped in plastic sheet and then in strong plastic sleeves prior to storage at 4˚C in the laboratory, although the upper 50cm were extruded and subsampled in the field owing to their high water content and unconsolidated nature. Alignment of ANTU1 and ANTU2 was achieved using stratigraphical and sedimentological markers (section 2.1, below).

1.2 Laboratory analyses

1.2.1 Water isotopes

Analyses were undertaken at the 'Lifer' stable isotope laboratory, Department of Earth, Ocean and Ecological Sciences, University of Liverpool.

H_2 gas was extracted from 2µL water samples by conventional high-temperature (500˚C) reduction in contact with Zn (Coleman et al. 1982; Horita & Kendall, 2004) in sealed, evacuated Pyrex tubes. Isotope ratios (δ^2H) were measured using a VG SIRA 12 mass spectrometer and their compositions reported in standard delta notation (‰), normalised to the VSMOW-SLAP scale (Coplen, 1988). Analytical precision was ±0.6 ‰.

Oxygen-isotope ratios ($\delta^{18}O$) were measured by standard CO_2 equilibration (Epstein & Mayeda, 1953; Horita & Kendall, 2004) of 2.5mL water samples at 25˚C for 48hr in a constant-temperature bath. After equilibration, the CO_2 was recovered cryogenically and analysed using a VG SIRA 10 mass spectrometer. Isotope ratios are reported in standard delta notation (in ‰), normalised to the VSMOW-SLAP scale (Coplen, 1988). Analytical precision was ±0.04 ‰.

The deuterium excess, d, for the modern water samples was calculated from the equation $d\ (‰) = \delta^2H - 8.\delta^{18}O$ (Dansgaard, 1964). This measures the degree of evaporation at the moisture source or the amount of evaporative enrichment during air-mass transportation to the precipitation site (Fröhlich et al., 2002). In continental environments, values ≤10‰ may indicate secondary evaporation processes, whereas recycling of water vapour from the surface may yield d-excess values >10‰ (Gat and Matsui, 1991; Gat et al., 1994).

1.2.2 Core stratigraphy and bulk-sediment composition

Apart from the upper 50cm, which were extruded and sampled in the field, the cores were opened in the laboratory, described and photographed. Subsamples were taken at stratigraphical resolution of 1 – 4 cm for determination of their bulk composition, extraction of material for dating, and analyses of TOC (total organic carbon), TN (total nitrogen), cellulose isotopes and lipid biomarkers. ~1 - 2g of wet sediment from each sample were dried for ≥12 hours at 105˚C to determine their water content, and then placed in a muffle furnace at 450˚C for 2hr, followed by 950˚C for 4hr, in order to estimate the bulk organic, carbonate and mineral fractions, respectively.

1.2.3 Cellulose extraction

The extraction of cellulose from lake sediments is based upon the standard chlorite method of Jayme and Wise for the isolation of cellulose from wood powder (Jayme, 1942; Wise et al., 1946), as reported in Green (1963) and Sternberg (1989a) and subsequently modified to take account of some of the additional constituents of sedimentary matrices (Edwards et al., 1997; Wolfe et al., 2001a,b).

Samples were treated with 1M (8-10% v/v) HCl to remove carbonates until the samples were acidic, washed with de-ionised water, freeze-dried (Thermo Savant ModulyoD, Thermo Fisher Scientific Inc.) and sieved using a 500µm sieve to remove macroscopic plant material and other debris. The coarse fraction was retained for future microscopic examination, including picking of aquatic mosses for separate isotope analysis. A solvent extraction using 2:1 toluene:ethanol was performed on the fine fraction to remove lipids, resins and tannin. In a novel step, these extracts were retained for GC-MS analysis. An additional solvent extraction was performed using acetone and the samples dried at room temperature. They were 'bleached' to remove lignin by *in situ* oxidation yielding chlorine dioxide (ClO_2) gas from the addition of glacial acetic acid and sodium chlorite. This procedure was repeated every hour until the sediment was grey/white (typically after 5-6 additions). An alkaline hydrolysis was then performed using 17% NaOH to remove xylan, mannan and other non-glucan polysaccharides (Loader et al., 1997). The samples were then treated with an oxyhydroxide leaching solution (sodium dithionite, tri-ammonium citrate and hydroxylamine hydrochloride) to remove any Fe and Mn oxyhydroxides. They were repeatedly mixed with the leaching solution and centrifuged until the supernatant was colourless. The resulting cellulose samples were washed 5-7 times with deionised water, frozen and freeze-dried.

1.2.4 Elemental and stable-isotope analyses

All analyses were undertaken at the Department of Geography, College of Science, Swansea University. Samples of lake sediment were analysed for total organic carbon (%TOC) and total nitrogen (%TN). ~1cm^3 of sediment was subsampled, dried and lightly crushed prior to removal of carbonates using excess dilute (5%) HCl. Samples were agitated and then allowed to stand for several hours until all carbonate had reacted (sample had stopped bubbling). Each sample was centrifuged and the acid decanted. They were then washed to neutrality with deionised water prior to freeze-drying (-48°C and 20mbar for 48h). Once dry, ~1mg subsamples of sediment were weighed into individual tin-foil capsules for elemental analysis.

Samples were combusted with excess O_2 over Cr(III) and Cu(II) oxides at 1000°C using a PDZ Europa ANCA GSL elemental analyser. The resulting sample gases were carried on a continuous flow of He through the combustion system. Excess oxygen, halogens and sulphur were removed by passing the resulting gases over hot Ag wire and hot Cu, which also reduced the oxides of nitrogen formed during combustion to N_2 gas. Traces of water were removed by passage through a magnesium perchlorate chemical water trap. The resulting N_2 and CO_2 gases were resolved gas-chromatographically using a 1.5m stainless steel GC column maintained at 70°C and packed with Porapack Q™ (McCarroll and Loader, 2004). TOC and TN were determined using a PDZ Europa 2020 isotope-ratio mass spectrometer and expressed relative to atropine and acetanilide standards (Loader et al. 2013). For stable carbon-isotope ($\delta^{13}C$) analysis, samples were either mass-corrected or weighed to yield a consistent CO_2 beam area roughly equivalent to 100µg of carbon. Carbon-isotope ratios were measured relative to the VPDB standard using acetanilide and in-house sigma cellulose standards (Loader et al., 2013) (Sigma Cellulose: Sigma Aldrich, UK, No. C-8002, Lot 92F-0243, with a measured value of -23.89 ± 0.12‰ σ_{n-1} (n = 951), which compares favourably with the analytical precision of the method typically reported (± 0.10‰ σ_{n-1}, n=10: McCarroll and Loader, 2004) prepared and analysed as described above. Typical analytical precision for repeat analyses of the acetanilide standard was ±0.90%, ±0.10%, and ±0.06 (σ_{n-1} n=26) for %TOC, %TN and C/N ratio, respectively.

Oxygen-isotope ratios were determined on samples of ~0.30-0.35mg of dry cellulose, weighed into silver-foil capsules and pyrolysed to CO gas at 1080°C over glassy carbon using a PDZ Europa ANCA GSL elemental analyser. The resulting CO was carried in a flow of He through an Ascarite CO_2 trap to remove any traces of the gas formed during pyrolysis at 1080°C and then through a magnesium perchlorate water trap to remove any traces of water formed during pyrolysis or during removal of CO_2 . The CO gas was resolved from any traces of N_2 gas chromatographically by passage through a 1m stainless steel column packed with a 5Å molecular sieve at 50°C (McCarroll and Loader 2004; Loader et al. 2008) Typical analytical precision was ± 0.3‰ (σ_{n-1}, n=10). Oxygen-isotope values of the cellulose source water ($\delta^{18}O_{lakewater}$) were estimated using the relationship $\delta^{18}O_{water} = 0.973 \times \delta^{18}O_{cellulose} - 27.2$ (Rozanski et al., 2010).

1.2.5 Lipid-biomarker analyses

The retained 2:1 toluene:ethanol solvent extracts were reduced in volume by rotary evaporation, transferred to weighed vials and taken to dryness under a stream of N_2. A known amount of standard (C_{36} *n*-alkane) was added to each sample prior to lipid analysis. Quantification and identification of *n*-alkanes and *n*-alkanoic acids was carried out by gas chromatography-mass spectrometry (GC–MS), performed using an Agilent 6890 gas chromatograph (split/splitless injection, 70 eV, EI) interfaced directly with an Agilent 5975 mass spectrometer. A HP5-MS fused silica capillary column (30 m × 0.25 mm; 0.25 µm

film thickness) was used. The oven temperature was held at 60°C for 1min, ramped at 10°C min^{-1} to 180 °C and then at 4°C min^{-1} to 300°C, where it was held for 15min. He was used as the carrier gas. Compounds were identified by comparison with known mass spectra, with published data and with the NIST Mass Spectral Library (version 2.0, 2005). The results were used to calculate the P_{alg} and P_{aq} proxies (refer to main text for details).

1.2.6 Endogenic carbonate analyses

Oxygen-isotope analyses of endogenic carbonate from core ANTU3 (refer to Fig. 1 in the main text for coring-site location), reported in Nedelskaja (2011) and supplemented with additional unpublished analyses, were compared with the cellulose oxygen-isotope data (section 3, below). Endogenic carbonate samples were dried at 105˚C and homogenized prior to stable-isotope analysis at the Department of Geology, Tallinn University of Technology, using a Thermo Fisher Scientific Delta V Advantage mass spectrometer and a GasBench II. Oxygen-isotope values are reported in standard delta notation relative to the VPDB standard, with uncertainties of ±0.1 ‰ for $\delta^{18}O$ (1σ).

2. The development of an age model for ANTU1 and ANTU2

2.1 Stratigraphical alignment of cores ANTU1 and ANTU2

Curves for organic carbon (estimated from loss-on-ignition at 450˚C, hereafter termed LOI) and carbonate (from loss-on-ignition at 950˚C, hereafter $CaCO_3$) show that ANTU2 is offset vertically from ANTU1 by -50cm (Figure S1).

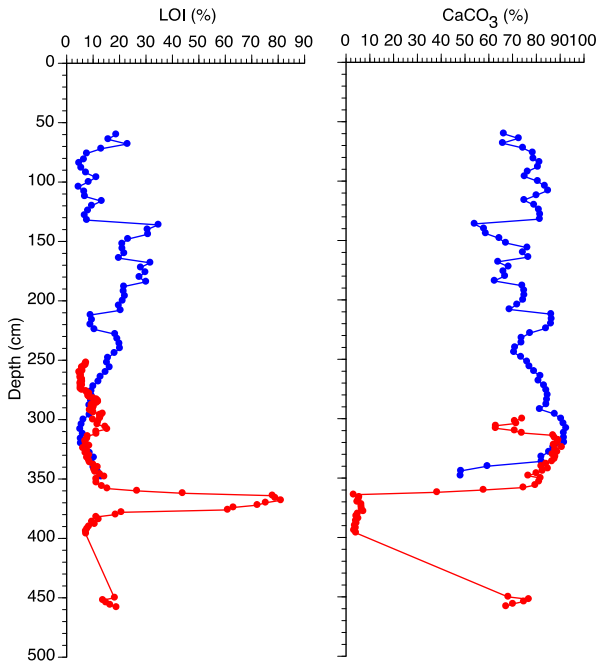

Fig. S1. Loss on ignition and carbonate content of cores ANTU1 (blue) and ANTU2 (red) plotted against original depth scales for each core.

A composite depth record (hereafter termed corrected depth) was therefore established from depth in ANTU1 and depth+50cm in ANTU2. LOI and $CaCO_3$ are plotted against corrected depth in Figure S2. A small gap exists in the carbonate record at the overlap between ANTU1 and ANTU2 because the $CaCO_3$ record does not extend as far up-sequence as the LOI record.

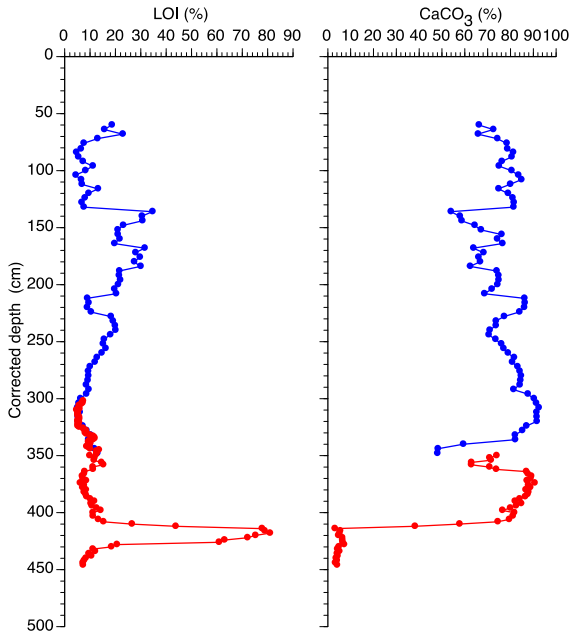

Fig. S2. LOI and $CaCO_3$ content of cores ANTU1 (blue) and ANTU2 (red) plotted against corrected depth.

The proposed stratigraphical alignment of ANTU1 and ANTU2 is supported by the visual stratigraphy of the two cores (Figure S3) and by the age-depth relationship, which is described in section 3 below. Although the visual stratigraphy suggests a slightly larger offset of ANTU2 (-50.5 cm), we preferred to use the value of 50cm based on LOI as this is likely to be more precise than visual matching.

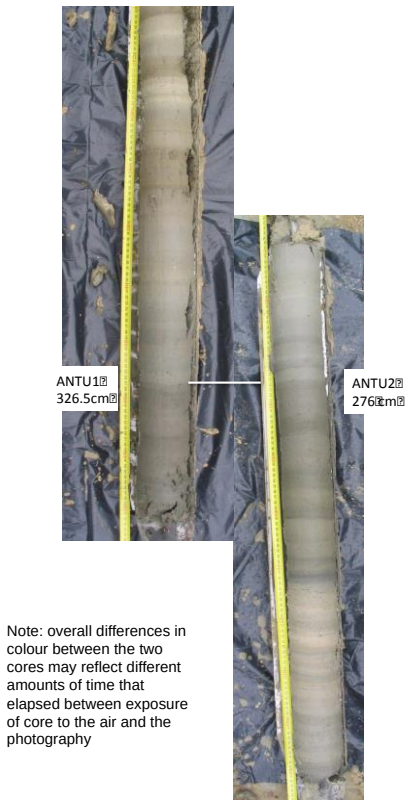

Fig. S3 Alignment of cores ANTU1 and ANTU2 based on visual stratigraphy.

2.2 Radiocarbon dates and age-depth relationship

The chronology for ANTU1 and ANTU2 is based on 8 radiocarbon dates (Table S1); terrestrial plant macrofossils were dated in order to avoid hardwater errors associated with aquatic material. Core samples were treated with 1M HCl to remove carbonate and rinsed with double distilled water, followed by wet sieving at 250µm and oven drying of the coarse fraction, from which macrofossils were picked under a low-power binocular microscope and transferred to clean, dry glass vials. Radiocarbon dating was performed at the SURRC AMS Facility, East Kilbride, Scotland.

Table S1. Radiocarbon dates for ANTU1 and ANTU2. Calibrations were performed using IntCal13 (Reimer et al., 2013).

Core	Depth (cm)^	Laboratory reference	Material	Radiocarbon age (^{14}C years BP)	Calendar age (years BP)	Age range (2s) (years BP)	$d^{13}C$ ‰ VPDB
ANTU1	147-148	SUERC-10878	Pinus cone	1629±35	1510	1414-1605	-27.8
ANTU1	258-259	SUERC-10879	Bark	4441±35	5080	4878-5281	-24.9
ANTU1	259-260	SUERC-10880	Bark	4583±35	5253	5059-5447	*-25
ANTU1	284-285	SUERC-10881	Pinus needles	5481±36	6300	6206-6393	-28.9
ANTU1	342-343	SUERC-10882	Pinus or Picea cone	7268±38	8089	8008-8170	-26.3
ANTU2	305-306	SUERC-10883	Bark	7938±46	8810	8635-8984	-28.6
ANTU2	307-308	SUERC-10884	Bark	8056±38	8930	8776-9083	-29.4
ANTU2	329-330	SUERC-10885	Pinus needles	8494±39	9501	9461-9540	-28.6

^Uncorrected depth

*estimated value, insufficient material for an independent measurement

A plot of calendar age against corrected depth (Fig. S4) provides further confirmation of our depth correction described above.

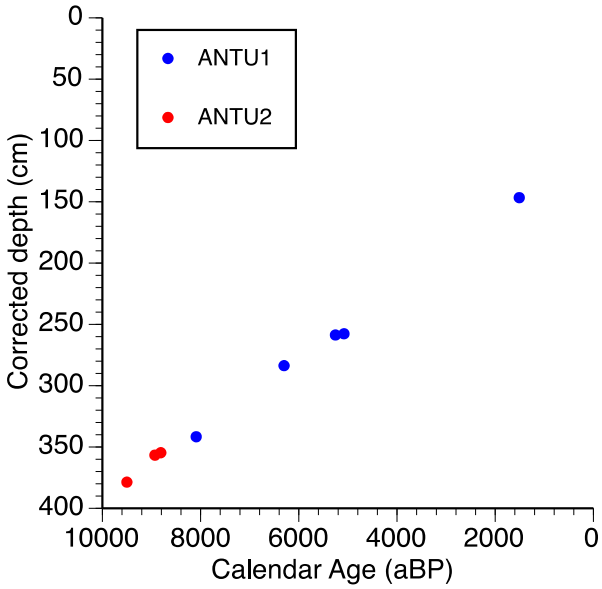

Fig. S4. Radiocarbon dates for ANTU1 and ANTU2. Dates have been calibrated using IntCal13 (Reimer et al., 2013) and are plotted against corrected depth.

2.3 Age constraint for the lower part of ANTU2

No plant macrofossils were found below 330 cm in ANTU2 (uncorrected depth), leaving the lower part of our sequence (prior to about 9500 cal. aBP) with no independent

chronological control. However, a radiocarbon date on terrestrial plant macrofossils from an additional core, ANTU3 (Nedelskaja, 2011), can be used to address this. Detailed LOI curves are not available for ANTU3. However, correlation between ANTU2 and ANTU3 was based on the pollen profiles for the two sequences (Fig. S5). In ANTU3 the oldest AMS dating based on terrestrial plant macrofossils (*Betula* seeds, unidentified bud scales) is 9340±60 BP at 511-516 cm (Poz-44780: Nedelskaja, 2011). The characteristics of the pollen assemblage of this level in the core (high content of *Betula* pollen, no pollen of *Alnus*, *Ulmus*, *Corylus*, and low herb content) allowed us to compare this with the pollen assemblage from ANTU2 core at the depth somewhere between 370-371 cm and 365-366cm.

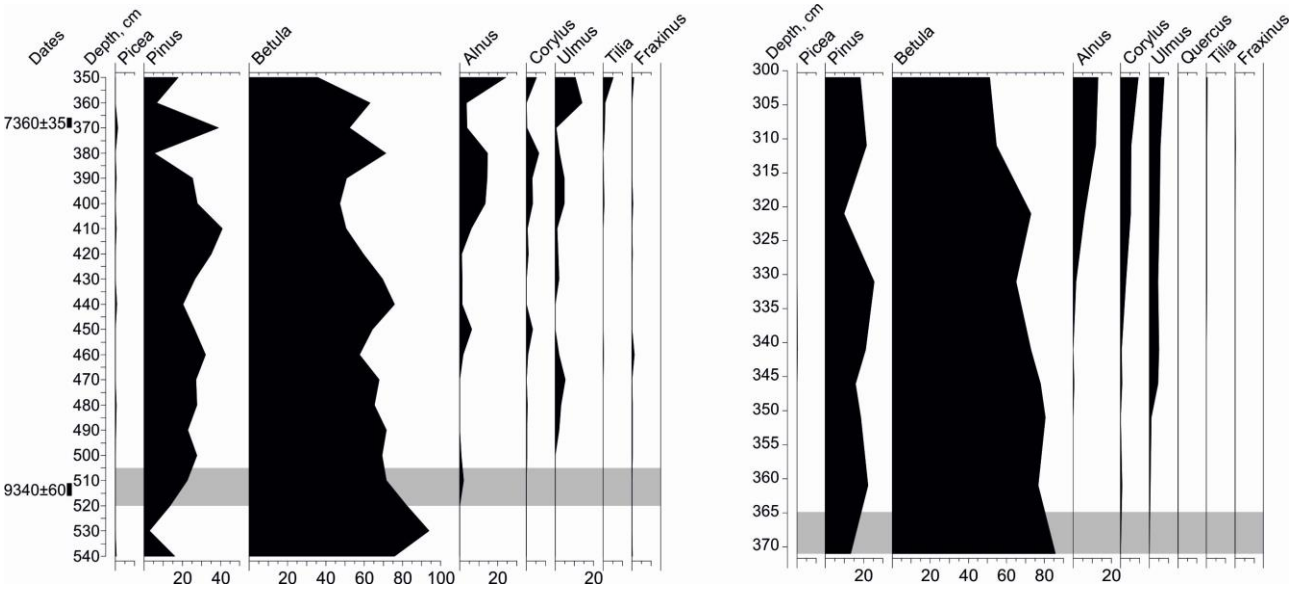

Fig. S5. Summary pollen profiles from ANTU3 (Nedelskaja, 2011) (left) and ANTU2 (right), showing proposed correlation (shaded interval)

We therefore used the date of 9340±60 BP, which is equivalent to a calendar age of 10301-10716 years BP, to provide additional age constraint for the lower part of ANTU1+2, choosing a depth of 368 cm (the median depth of the proposed level of correlation), which is equivalent to a corrected depth of 418 cm (Fig. S6).

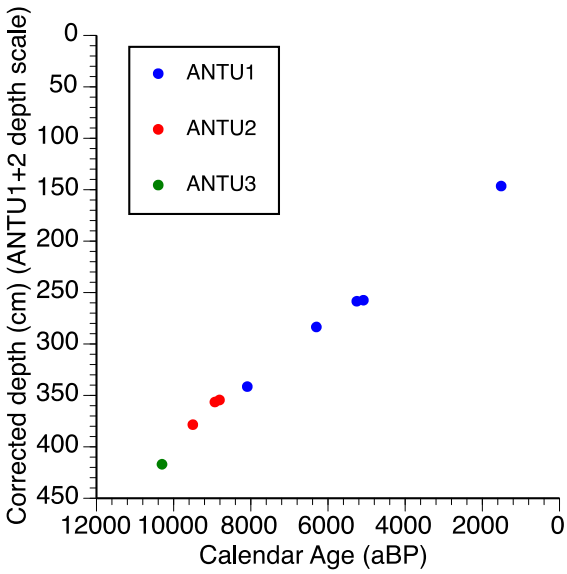

Fig. S6. Composite age-depth relationship for ANTU1 and ANTU2, including the date from ANTU3. Dates have been calibrated and are plotted against corrected depth.

2.4 Age modelling

Radiocarbon dates were calibrated using IntCal13 (Reimer et al., 2013); classical age-depth modelling was undertaken using Clam 2.2 (Blaauw, 2010) and an age model provided by a smooth spline (Fig. S7).

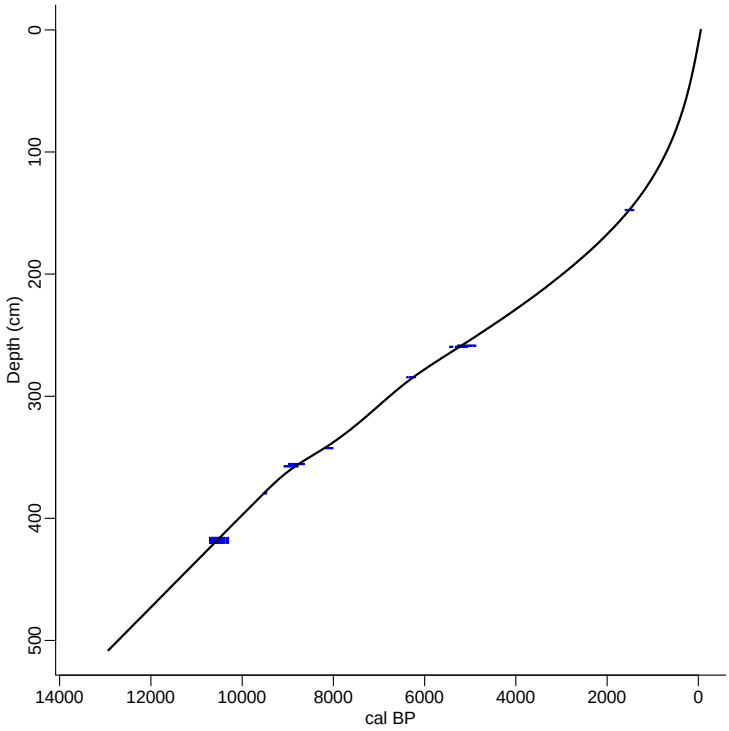

Fig. S7. Age – depth pairs for ANTU 1 and 2, versus 'corrected' depth and described by a smooth spline. Shading represents 95% confidence intervals.

3. Isotope-derived Holocene palaeotemperatures for Äntu Sinijärv

Holocene variations in temperature at Lake Äntu Sinijärv were estimated using the modern relationship between $\delta^{18}O_{mw}$ and mean annual air temperature (MAT) values to convert $\delta^{18}O_{lakewater}$ values to MAT (cf. Edwards et al. 1996; von Grafenstein et al., 1996).

$\delta^{18}O_{lakewater}$ values were calculated from $\delta^{18}O_{cellulose}$, as described in section 1.24, above. The cellulose was assumed to be aquatic in origin and the fractionation between cellulose and water temperature-independent (Barbour et al., 2001; Roden et al., 2000; Sternberg et al., 1986). Lake water in Äntu Sinijärv, which is a small and well-mixed lake with a short residence time and limited seasonal isotopic variability, is negligibly modified by evaporative enrichment and deemed to approximate the isotopic composition of regional groundwater, which in turn is closely related to the isotopic composition of weighted mean annual $\delta^{18}O_{mw}$. The oxygen-isotope composition of local rainfall, as represented by the GNIP station at Tartu, is related to air temperature by the equation $T = 2.1\ \delta^{18}O + 30.1$ (Fig. S8). The modern annual MAT estimated by this method (+4.5 to +5.95˚C) agrees closely with the observed value (+4.9˚C).

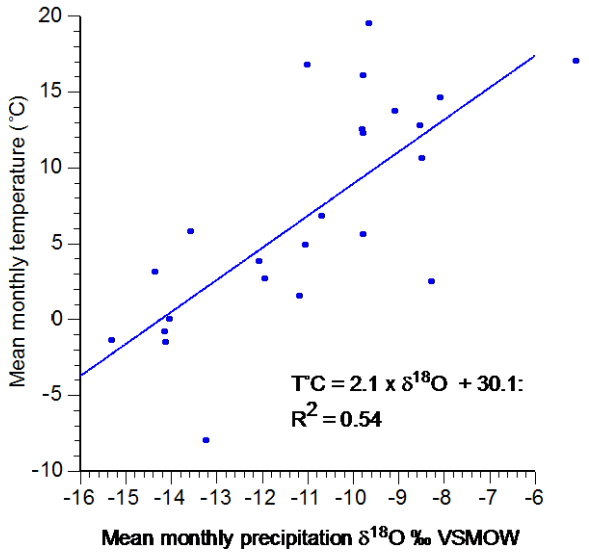

Fig. S8. Monthly precipitation from Tartu against monthly air temperature, January 2014 – December 2015 (IAEA/WMO, 2017).

The reconstructed temperatures and inferred $\delta^{18}O_{lakewater}$ values from core ANTU1+2 were also used to calculate 'predicted' $\delta^{18}O_{carbonate}$ values using the equation of Kim and O'Neil (1997), assuming isotopic equilibrium between calcite and water. The 'predicted' values were then compared with the measured $\delta^{18}O_{carbonate}$ values from ANTU3 (section 1.2.6 above: see main text for further discussion). Ages for the measured $\delta^{18}O_{carbonate}$ values were interpolated between the radiocarbon dates for ANTU3 (Nedelskaja, 2011).

References

Barbour, M.M., Andrews, T.J. and Farquhar, G.D. 2001. Correlations between oxygen isotope ratios of wood constituents of *Quercus* and *Pinus* samples from around the world. Australian Journal of Plant Physiology 28, 335–348.

Blaauw, M. 2010. Methods and code for 'classical' age-modelling of radiocarbon sequences. Quaternary Geochronology, 5, 512-518.

Coleman, M.L., Shepherd, T.J., Durham, J.J., Rouse, J.E. and Moore, G.R. 1982. Reduction of water with zinc for hydrogen isotope analysis. Analytical Chemistry, 54, 993-995.

Coplen, T.B. 1988. Normalization of oxygen and hydrogen isotope data. Chemical Geology, 72, 293-297.

Craig, H. 1961. Isotopic variations in meteoric waters. Science, 133, 1702-1703.

Dansgaard, W. 1964. Stable isotopes in precipitation. Tellus, 16, 436-468.

Edwards, T.W.D., Elgood, R.J. and Wolfe, B.B. 1997. Cellulose extraction from lake sediments for $^{18}O/^{16}O$ and $^{13}C/^{12}C$ analysis. Technical Procedure 28.0. Waterloo, Canada: Environmental Isotope Laboratory, Department of Earth Sciences, University of Waterloo, pp. 4.

Edwards, T.W.D., Wolfe, B.B. and MacDonald, G.M. 1996. Influence of changing atmospheric circulation on precipitation $\delta^{18}O$-temperature relations in Canada during the Holocene. Quaternary Research, 46, 211-218.

Epstein, S. and Mayeda, T.K. 1953. Variations of O^{18} of waters from natural sources. Geochimica et Cosmochimica Acta, 4, 213-224.

Fröhlich, K., Gibson, J.J. and Aggarwal, P.K. 2002. Deuterium excess in precipitation and its climatological significance, Study of Environmental Change using Isotope Techniques. International Atomic Energy Agency, International Conference in Vienna, Austria, 23-27 April 2001, pp. 54-65.

Gat, J.R., Bowser, C.J. and Kendall, C. 1994. The contribution of evaporation from the Great Lakes to the continental atmosphere: estimate based on stable isotope data. Geophysical Research Letters, 21, 557-560.

Gat, J.R. and Matsui, E., 1991. Atmospheric water balance in the Amazon Basin: an isotopic evapotranspiration model. Journal of Geophysical Research, 96, 13179-113188.

Green, J. W., 1963. Wood cellulose. In: Whistler, R. L. (ed.) Methods in Carbohydrate Chemistry, Vol. III. Academic Press, New York: 9–20.

Horita, J. and Kendall, C. 2004. Stable isotope analysis of water and aqueous solutions by conventional dual-inlet mass spectrometry. In: de Groot, P.A. (ed.) Handbook of Stable Isotope Analytical Techniques, Volume 1, 1-37.

IAEA/WMO 2017. Global Network of Isotopes in Precipitation. The GNIP Database. Accessible at: http://www.iaea.org/water. Accessed 16 August 2017.

Jayme, G. 1942. Cellulosechemie, 20, 43

Keatings K.W., Heaton T.H.E. and Holmes J.A. 2002. Carbon and oxygen isotope fractionation in non-marine ostracods: Results from a 'natural culture' environment. Geochimica et Cosmochimica Acta, 66,1701-1711.

Kim, S.T. and O'Neil, J.R. 1997. Equilibrium and nonequilibrium oxygen isotope effects in synthetic carbonates. Geochimica et Cosmochimica Acta, 61, 3461-3475.

Loader, N.J., Robertson, I., Barker, A.C., Switsur, V.R. and Waterhouse, J.S. 1997. An improved technique for the batch processing of small wholewood samples to α-cellulose. Chemical Geology, 136, 313-317.

Loader, N.J., Young, G.H.F., Grudd, H. and McCarroll, D. 2013. Stable carbon isotopes from Torneträsk, northern Sweden provide a millennial length reconstruction of summer sunshine and its relationship to Arctic circulation. Quaternary Science Reviews, 62, 97–113.

McCarroll, D., and Loader, N.J. 2004. Stable isotopes in tree-rings. Quaternary Science Reviews, 23, 765–778.

Nedelskaja, A. 2011. Õietolmuspektrite ning hapniku ja süsiniku isotoop-andmete analüüs mõnede Eesti väikejärvede setetes. MSc Thesis, Tallinn University, Estonia.

Paillard, D., Labeyrie L. and Yiou, P. 1996. Macintosh program performs time-series analysis, Eos Tranactions American Geophysical Union, 77, 379.

Reimer, P. J., Bard, E., Bayliss, A., Beck, J. W., Blackwell, P. G., Ramsey, C. B., Buck, C. E., Cheng, H., Edwards, R. L., Friedrich, M., Grootes, P. M., Guilderson, T. P., Haflidason, H., Hajdas, I., Hatte, C., Heaton, T. J., Hoffmann, D. L., Hogg, A. G., Hughen, K. A., Kaiser, K. F., Kromer, B., Manning, S. W., Niu, M., Reimer, R. W., Richards, D. A., Scott, E. M., Southon, J. R., Staff, R. A., Turney, C. S. M. and van der Plicht, J. 2013. Intcal13 and Marine13 radiocarbon age calibration curves 0-50,000 Years Cal BP. Radiocarbon, 55, 1869-1887.

Roden, J.S., Lin, G. and Ehleringer, J.R., 2000. A mechanistic model for interpretation of hydrogen and oxygen isotope ratios in tree-ring cellulose. Geochimica et Cosmochimica Acta, 64, 21–35.

Rozanski, K., Klisch, M.A., Wachniew, P., Gorczyca, Z., Goslar, T., Edwards, T.W.D. and Shemesh, A. 2010. Oxygen-isotope geothermometers in lacustrine sediments: New insights through combined $\delta^{18}O$ analyses of aquatic cellulose, authigenic calcite and biogenic silica in Lake Gościąż, central Poland. Geochimica et Cosmochimica Acta, 74, 2957-2969.

Sternberg, L. da S.L. 1989a. Oxygen and hydrogen isotope measurements in plant cellulose analysis. In: Linskens, H.F. and Jackson, J.F. (eds.) Plant Fibers. New York: Springer-Verlag. pp.89-99.

Sternberg, L. da S.L. 1989b. Oxygen and hydrogen isotope ratios in plant cellulose: mechanisms and applications. In: Rundel, P.W., Ehleringer, J.R. and Nagy, K.A. (eds.) Stable Isotopes in Ecological Research. Ecological Studies, Vol. 68. New York: Springer-Verlag. pp.124-141.

Sternberg, L., De Niro, M. and Savidge, R. 1986. Oxygen isotope exchange between metabolites and water during biochemical reactions leading to cellulose synthesis. Plant Physiology, 82, 423–427.

von Grafenstein U., Erlernkeuser H. and Trimborn P. 1999. Oxygen and carbon isotopes in modern fresh-water ostracod valves: assessing vital offsets and autecological effects of interest for palaeoclimate studies. Palaeogeography, Palaeoclimatology, Palaeoecology, 148, 133-152.

von Grafenstein, U., Erlenkeuser, H., Müller, J., Trimborn, P. and Alefs, J. 1996. A 200 year mid-European air temperature record preserved in lake sediments: An extension of the $\delta^{18}O_p$-air temperature relation into the past. Geochimica et Cosmochimica Acta, 60, 4025-4036.

Wise, L.E., Murphy, M. and D'Addieco, A.A. 1946. Paper Trade Journal, 122, 35.

Wolfe B.B., Aravena, R., Abbott, M.B., Seltzer, G.O. and Gibson, J.J. 2001. Reconstruction of paleohydrology and paleohumidity from oxygen isotope records in the Bolivian Andes. Palaeogeography, Palaeoclimatology, Palaeoecology 176, 177-192.

Wolfe, B.B., Edwards, T.W.D., Beuning, K.R.M. and Elgood, R.J. 2001. Carbon and oxygen isotope analysis of lake sediment cellulose: methods and applications. In: Last, W. M. and Smol. J.P. (eds.) Tracking Environmental Change Using Lake Sediments: Physical and Chemical Techniques, Developments in Paleoenvironmental Research, Vol. 2. Kluwer Academic Publishers, Dordrecht, The Netherlands, pp. 373-400.